ACS Medicinal Chemistry Letters

Letter

Cite This: ACS Med. Chem. Lett. 2019, 10, 1486−1491

pubs.acs.org/acsmedchemlett

Discovery of Pyridazinone and Pyrazolo[1,5-*a*]pyridine Inhibitors of C-Terminal Src Kinase

Daniel P. O'Malley,* Vijay Ahuja, Brian Fink, Carolyn Cao, Cindy Wang, Jesse Swanson, Susan Wee, Ashvinikumar V. Gavai, John Tokarski, David Critton, Anthony A. Paiva, Benjamin M. Johnson, Nicolas Szapiel, and Dianlin Xie

Bristol-Myers Squibb Company, Research and Development, Route 206 and Province Line Road, Princeton, New Jersey 08543, United States

Supporting Information

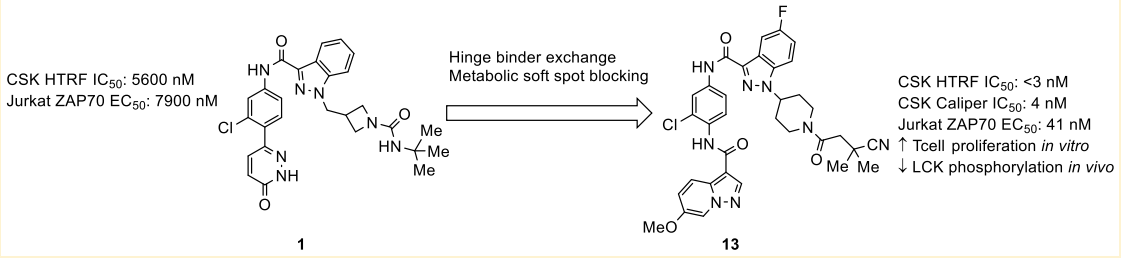

ABSTRACT: C-terminal Src kinase (CSK) functions as a negative regulator of T cell activation through inhibitory phosphorylation of LCK, so inhibitors of CSK are of interest as potential immuno-oncology agents. Screening of an internal kinase inhibitor collection identified pyridazinone lead **1**, and a series of modifications led to optimized compound **13**. Compound **13** showed potent activity in biochemical and cellular assays *in vitro* and demonstrated the ability to increase T cell proliferation induced by T cell receptor signaling. Compound **13** gave extended exposure in mice upon oral dosing and produced a functional response (decrease in LCK phosphorylation) in mouse spleens at 6 h post dose.

KEYWORDS: *CSK inhibitor, kinase inhibitor, immuno-oncology, Metabolite ID*

The development of antibodies targeting CTLA-4, PD-1, and PD-L1 to activate the immune system holds great promise for the treatment of cancer. Although these treatments offer substantial therapeutic benefit, as reflected by their recent approval for the treatment of melanoma, nonsmall cell lung cancer, renal cell carcinoma, and a number of other indications, there remains a population of patients that do not respond to currently available immuno-oncology agents. There is consequently a critical need for additional agents to help extend the benefits of immunotherapy to additional patients and indications.[1−3]

In T cells, the SRC-family kinase LCK plays a key role in initiating the proximal T cell receptor pathway by phosphorylating the ξ and CD3 chains of the T cell receptor, as well as downstream kinases such as ZAP-70.[4] LCK is in turn negatively regulated by phosphorylation on Tyr505 by c-terminal SRC kinase (CSK), which causes LCK to adopt its closed, inactive conformation.[5−7] Inhibition of CSK could therefore augment T cell activation in response to antigen recognition by the T cell receptor by retaining LCK in an activated form. Indeed, siRNA knockdown of CSK in primary T cells and Jurkat cells increases LCK signaling and response to T cell receptor stimulation.[8] Studies in transgenic mice expressing a variant of CSK engineered to be sensitive to chemical inhibition have demonstrated that this inhibition increases the response of T cells to weak antigens.[9] In addition, both CSK and LCK have been shown to associate with PD-1, and PD-1 activation has been shown to reduce ZAP-70 phosphorylation, indicating that CSK inhibition could synergize with anti-PD-1/PD-L1 therapy.[10,11] To date, there have been no reports of potent small molecule CSK inhibitors.[12] The development of suitable tool molecules to evaluate the potential to activate T cells through CSK inhibition is therefore of great interest.

Screening of an internal kinase inhibitor collection identified compound **1** (Figure 1) as a starting point for optimization. Despite its modest potency in a CSK HTRF binding assay (Table 1), this compound increased ZAP-70 phosphorylation in Jurkat cells and had no measurable LCK activity. As the ultimate aim of inhibiting CSK was the enhancement of LCK activity, selectivity for inhibition of CSK over LCK was considered highly important. Although the two proteins are only 44% identical in their kinase domains, only two of the residues facing the ATP-binding pocket differ (Leu251 and Ala381 in Lck), complicating attempts to obtain selective inhibitors. The initial goals for optimization were to improve

Received: August 1, 2019
Accepted: September 25, 2019
Published: September 25, 2019

DOI: 10.1021/acsmedchemlett.9b00354
ACS Med. Chem. Lett. 2019, 10, 1486−1491

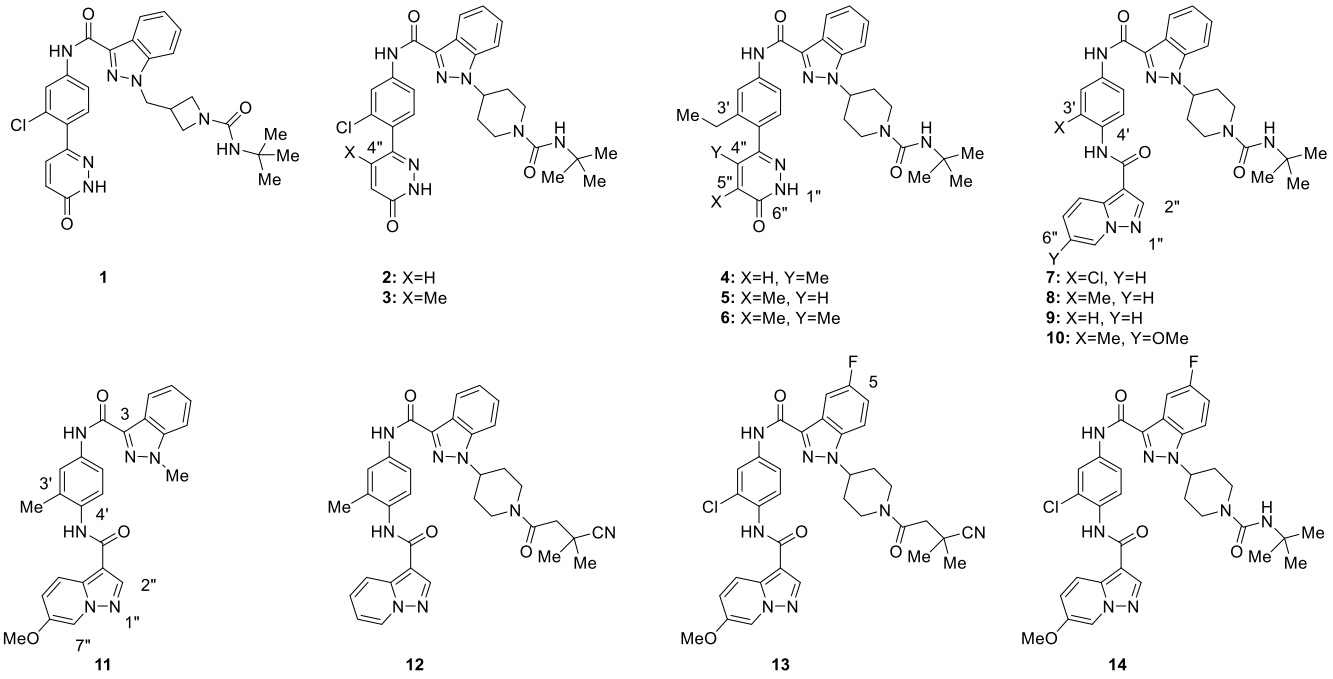

Figure 1. Structures of CSK inhibitors **1**−**14**.

Table 1. Characterization of CSK Inhibitors 1−6[a,b]

Cpd	CSK IC_{50} (nM)	LCK IC_{50} (nM)	ZAP-70 EC_{50} (nM) (Y_{max})	HLM/MsLM %Rem.
1	5600	>50000	7900(73%)	2/33
2	79	24000	5700(180%)	65/15
3	80	31000	4050(350%)	68/9
4	70	43000	2000(350%)	53/78
5	430	34000	2700(280%)	72/1
6	8	26000	420(270%)	61/59

[a]For assay conditions and replicate numbers, see the Supporting Information [b]HLM: Human liver microsomes. MsLM: Mouse liver microsomes.%Rem: Percent remaining at 10 min.

Table 2. Characterization of CSK Inhibitors 7−14[a,b]

Cpd	CSK IC_{50} (nM) HTRF	CSK IC_{50} (nM) Caliper	LCK IC_{50} (nM)	ZAP-70 EC_{50} (nM) (Y_{max})	HLM/MsLM %Rem
7	5	4	300	49(250%)	84/24
8	<3	4	120	42(190%)	72/10
9	26	21	3100	1400(240%)	71/21
10	<3	2	26	28(220%)	80/2
11	42	13	42	>20000	NT/59
12	<3	4	230	88(370%)	85/9
13	<3	4	260	41(360%)	91/100
14	4	6	110	56(210%)	85/99

[a]For assay conditions and replicate numbers, see the Supporting Information [b]NT: not tested.

potency in the binding and cellular assays and to improve the low metabolic stability in human and mouse liver microsomes, while maintaining selectivity against LCK.

Since structural information regarding the binding of **1** to CSK was not available at the outset of the project, initial optimization efforts focused on introducing conformational biases as a means to enhance potency. The azetidinylmethyl group in **1** was replaced with a piperidine (compound **2**) based

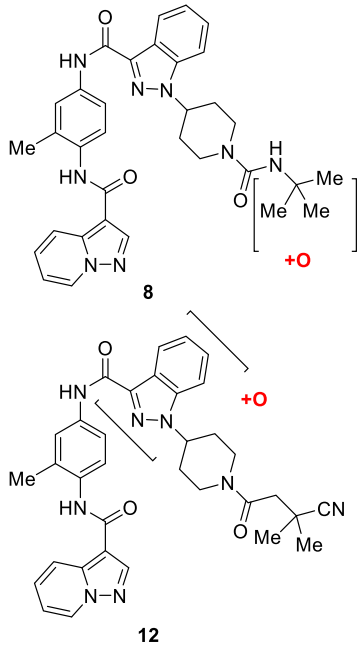

Figure 2. Sites of metabolism of compounds **8** and **12**.

on the hypothesis that this would reduce conformational flexibility and favor the necessary orientation of the urea group. This resulted in a substantial increase in CSK potency and improvement in human metabolic stability, although the increase in cellular potency was modest and mouse metabolic stability remained low.

An attempt to bias the conformation of the biaryl junction to favor a nonplanar orientation by introduction of a methyl group at C4′′ of the pyridazinone (**3**) resulted in a similar profile, as did replacement of the C3′ chloro substituent on the phenyl ring with a larger ethyl group (**4**). Movement of the C4′′ methyl to C5′′ (**5**) caused a slight drop in potency; incorporation of methyl groups at both positions (**6**) gave a

DOI: 10.1021/acsmedchemlett.9b00354
ACS Med. Chem. Lett. 2019, 10, 1486−1491

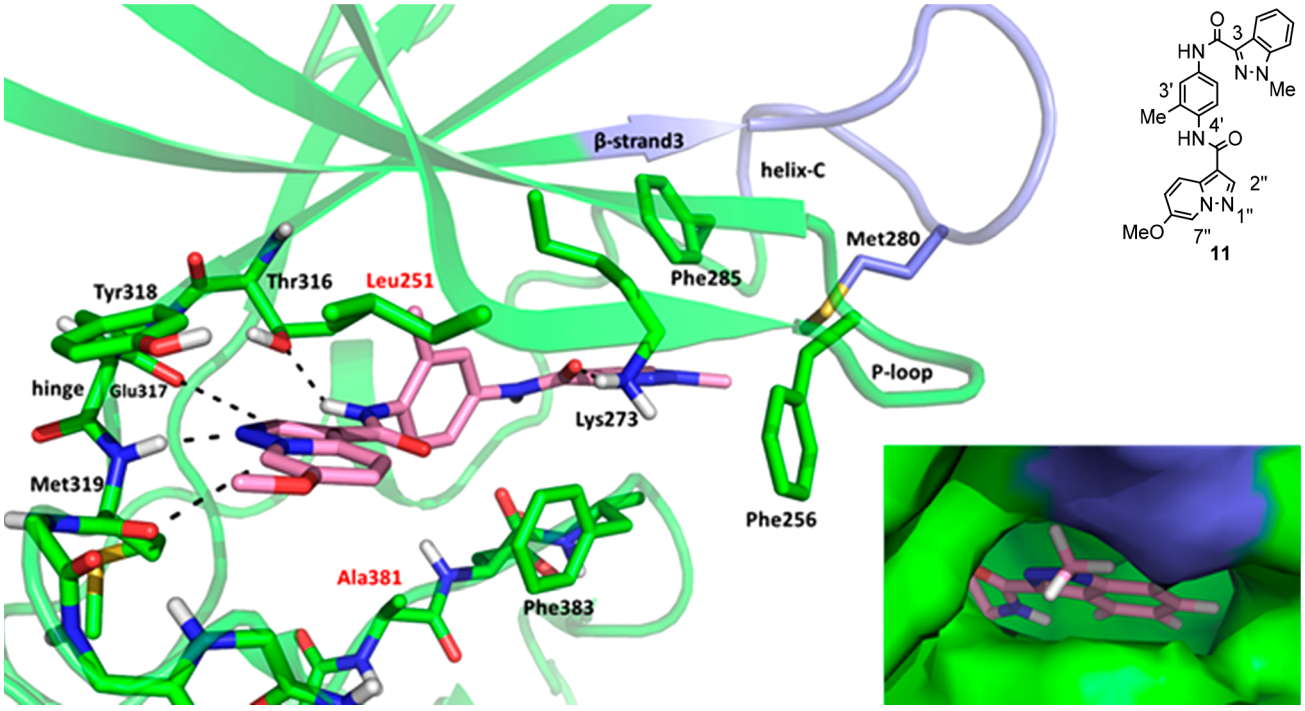

Figure 3. X-ray structure of LCK and **11**. Hydrogen bonds and favorable interactions are denoted with dashes. The carbons and ribbon representation of LCK are colored green except for the loop between β-strand3 and helix-C which is colored blue. The carbons of **11** are colored pink, oxygen is red, and nitrogen is blue. Residues in the binding pocket that differ between LCK and CSK have red labels. Bottom right: Close-up of the surface of LCK around the indazole. The surface of LCK is colored green except for the loop between the β-strand3 and helix-C which is colored blue.

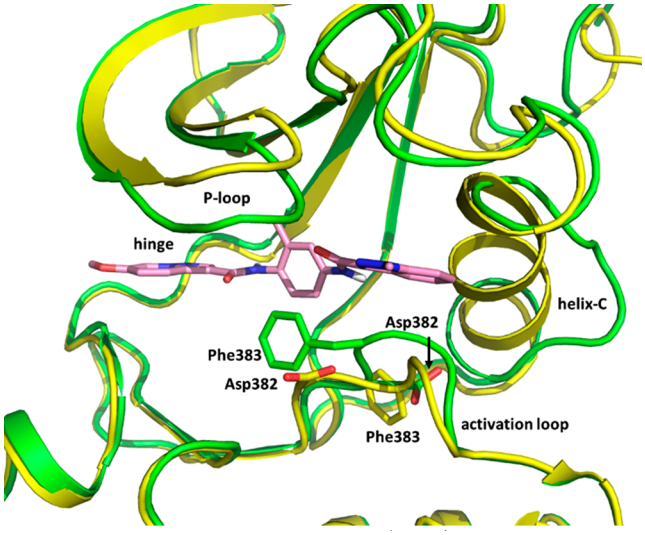

Figure 4. X-ray structures of LCK and **11** (green) superposed with apo LCK (yellow, PDB code 3LCK) highlighting the residues of the DFG motif. The carbons of **11** are colored pink.

moderate increase in both binding and cellular potency. Interestingly, compounds containing both the C3′ ethyl and C4′′ methyl groups (**4** and **6**) showed substantially increased mouse metabolic stability, whereas compounds containing only one of the two groups (**3** and **5**) did not.

Unfortunately, efforts to further increase potency by straightforward modification of compound **6** proved unfruitful, so attempts were made to replace the pyridazinone with a series of other groups that had the potential to maintain a similar pattern of hydrogen bonding interactions. This approach was validated by compound **7**, which was designed based on the hypothesis that N1′′ and the C2′′ hydrogen of the pyrazolopyridine would occupy a similar location to the C6′′ carbonyl and N1′′ hydrogen of pyridazinone **6**. This compound had an IC_{50} value of 5 nM in the CSK HTRF assay and EC_{50} of 49 nM in the cellular ZAP-70 assay (Table 2); since compounds in this series often had IC_{50} values below 3 nM in the CSK HTRF assay (the lower limit of the assay), they were also tested in a Caliper assay to give a more precise measurement of their potency.

Investigation of the C3′ chloro substituent revealed that replacement with a methyl group (compound **8**) maintained potency, while its removal (**9**) resulted in a decrease in both biochemical and cellular potency. This result suggested that this group plays an important role through direct interaction with CSK and/or influence on the conformation of the C4′ amide bond. An attempt to improve potency by introduction of a methoxy group at C6′′ (**10**) had minimal effect on CSK potency but did cause an undesired increase in LCK potency. Despite this, compound **10** maintained activity in the cellular assay, indicating that even a relatively low level of selectivity for CSK over LCK may be sufficient in a cellular context.

Despite the exciting levels of potency shown by these compounds, their poor mouse metabolic stability prevented their use in animal studies. In an attempt to remove potential sites of metabolism on the substituted piperidine, compound **11**, in which this substituent has been truncated to a methyl group, was prepared. Although **11** did show an increase in mouse metabolic stability, it also had lower CSK potency and did not show cellular activity.

In order to ascertain the location of its metabolic vulnerabilities, metabolism of compound **8** by mouse liver

DOI: 10.1021/acsmedchemlett.9b00354
ACS Med. Chem. Lett. 2019, 10, 1486−1491

Scheme 1. Synthesis of Compound 8[a]

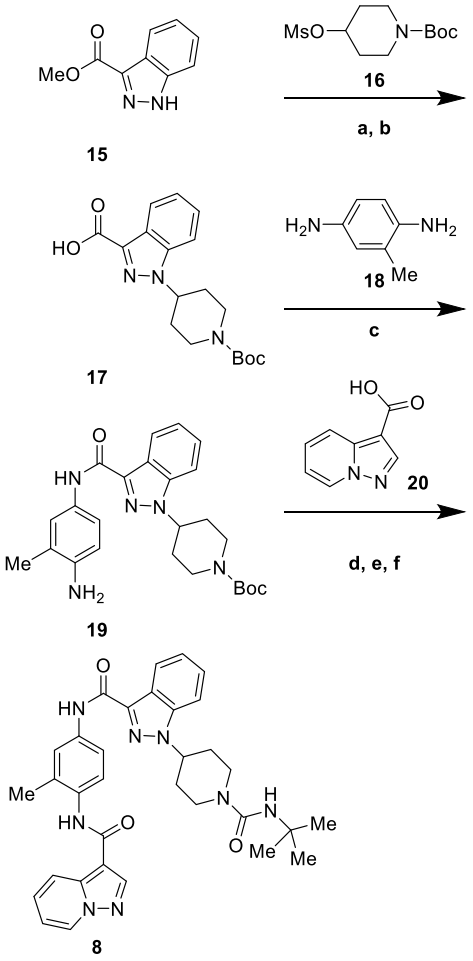

[a]Reagents and conditions: (a) **16**, Cs_2CO_3, DMF, 80 °C, 39%; (b) LiOH, MeOH, H_2O, quant.; (c) **18**, PyBOP, Hünig's base, DMF, 79%; (d) **20**, PyBOP, Hünig's base, THF, rt to 60 °C, 47%; (e) HCl, dioxane, quant.; (f) *tert*-butyl isocyanate, Hünig's base, DMF, 41%.

microsomes was studied and oxidation of the *tert*-butyl group was identified as the sole metabolite (Figure 2).[13]

This knowledge spurred attempts to block metabolism of the *tert*-butyl group by replacing it with a series of groups containing polar and electron-withdrawing substituents. Although this yielded compounds that maintained the high level of potency shown by **8**, these compounds did not show the expected increase in metabolic stability, as typified by cyano amide **12**. Analysis of the metabolism of compound **12** revealed a new site of metabolism, oxidation of the indazole ring. Attempts were made to block this by fluorination of the indazole ring; the C-5 fluoro derivative **13** showed a dramatic improvement in metabolic stability combined with good biochemical and cellular potency. Interestingly, compound **14**, which contains the fluoroindazole but maintains the *tert*-butyl urea that had proved to be metabolically labile in other analogs, also showed improved metabolic stability. This suggests that the role of the fluorine on the indazole extends beyond simply preventing oxidation of the indazole through local steric or electronic effects, possibly by creating an unfavorable interaction with the metabolizing enzyme.

In an attempt to understand the binding mode of these chemotypes, efforts were made to obtain crystal structures with

Scheme 2. Synthesis of Compound 4[a]

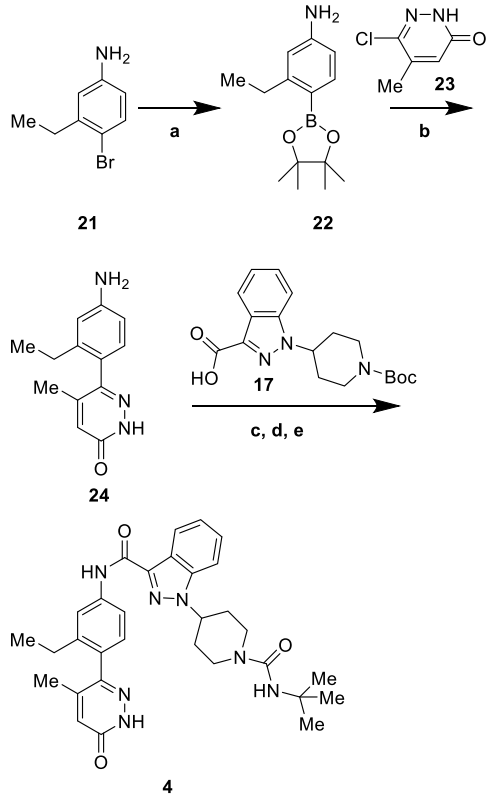

[a]Reagents and conditions: (a) $PdCl_2$(dppf)·DCM, bis(pinacolato)-diboron, KOAc, dioxane, 100 °C, 39%; (b) **23**, $PdCl_2$(dppf)·DCM, Na_2CO_3, DMF, H_2O, 35%; (c) **17**, PyBOP, Hünig's base, DMF, 67%; (d) HCl, dioxane, quant.; (e) *tert*-butyl isocyanate, Hünig's base, DCM, 67%.

Table 3. Further Profiling of Compounds 4, 6, 13, and 14[a,b]

Cpd	HLM $T_{1/2}$ (min)	MsLM $T_{1/2}$ (min)	Human PB %Free	Mouse PB %Free	FSI(100)
4	10	31	0.4%	0.9%	5.5
6	14	12	0.5%	1.0%	3.0
13	>120	>120	<0.1%	0.3%	6.7
14	>120	88	0.4%	<0.2%	8.9

[a]PB: protein binding. [b]FSI(100): percent of 238 kinases tested in an internal panel with an IC_{50} value within 100-fold of the compound's CSK HTRF IC_{50}.

Table 4. PK and PD Parameters for Compounds 4 and 13[a]

Cpd	C_{max} (μM)	T_{max} (h)	C_{24h} (μM)	AUC (μM·h)	$T_{1/2}$ (h)	ΔLCK pY505
4	17.3	0.3	0.001	51.5	1.9	−87%
13	19.3	7	1.3	221.5	5.3	−88%

[a]ΔLCK pY505: percent change in LCK pY505 compared to vehicle, t = 3 h for **4**, t = 6 h for **13**. C57bl/6 mice were used.

several compounds. Although no usable crystal structures were obtained with CSK, a structure of **11** in complex with LCK was obtained (Figure 3). The structure reveals that **11** sits in the ATP binding site and makes hydrogen bonds from N1′′ of the pyrazolopyridine ring to the hinge backbone NH of Met319 and from the amide NH at C4′ to the side chain hydroxyl oxygen of Thr316. In addition, the distance between C7′′ of the pyrazolopyridine and the backbone carbonyl oxygen of

DOI: 10.1021/acsmedchemlett.9b00354
ACS Med. Chem. Lett. 2019, 10, 1486−1491

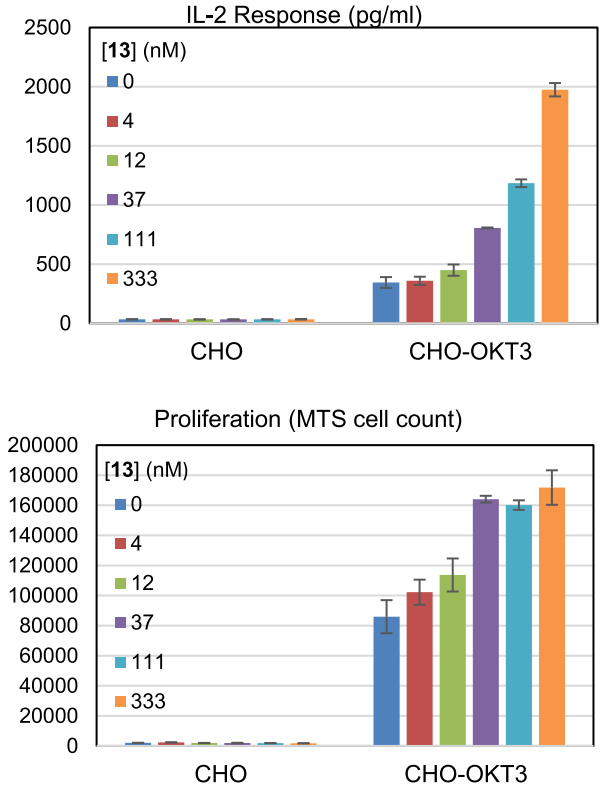

Figure 5. Top: $CD4^+$ T cell IL-2 secretion in response to **13**. Bottom: $CD4^+$ T cell proliferation in response to **13**.

Met319 is 3.1 Å and the distance between C2′′ of the backbone oxygen of Glu317 is 3.5 Å, indicating the presence of favorable binding interactions between these residues and **11**. The amide carbonyl oxygen at C3 of the indazole ring makes a hydrogen bond with the side chain of Lys273.

The C3′ methyl of the phenyl ring points into a small pocket below β-strand 3 and contributes to the nonplanarity of the phenyl ring relative to the amide. This likely explains the decrease in potency observed in compound **9** as compared to **7** and **8**. The indazole ring forms an edge-to-face interaction with Phe285 and has a lipophilic interaction with Met280. Comparison of the structure of LCK with **11** bound to the apo structure (Figure 4) shows that **11** binds in an inactive DFG-out conformation, with significant distortion of helix C.

It is noteworthy that the N1 methyl group in compound **11** points toward the loop between β-strand 3 and α-helix C. Analysis of the protein surface in this area (Figure 1 inset) shows relatively little space to accommodate substituents larger than this methyl group, and compounds containing a substituted piperidine at this position show increased selectivity for CSK relative to **11**. This region of LCK shares little homology with CSK, so this increased selectivity is likely attributable to an increased ability of the corresponding region of CSK to make favorable interactions with substituents larger than methyl. The N1 substituent is not in proximity to Leu251 or Ala381, the two residues in the binding pocket that are different in CSK (corresponding to Ile201 and Ser331, respectively), so the sequence differences in the loop between β-strand 3 and α-helix C are likely the major contributor to selectivity between LCK and CSK.

Illustrative syntheses of compounds **8** and **4** are shown in Schemes 1 and 2. Alkylation of indazole **15** with mesylate **16** followed by ester hydrolysis gave carboxylic acid **17**. Acylation of bis-aniline **18** with this acid occurred primarily at the less hindered amine to give **19**, which was then acylated a second time with acid **20.**

Removal of the Boc group and installation of the *tert*-butyl urea with *tert*-butyl isocyanate completed the synthesis of compound **8**. For the preparation of **4** (Scheme 2), bromide **21** was converted to boronic ester **22**, which was then coupled to choloropyridazinone **23** to give **24**. Coupling with acid **17** was effected with PyBOP; the choice of coupling reagents was important, as reagents such as HATU had a tendency to form adducts with unprotected pyridazinones such as **24** and its coupled product. Synthesis of **4** was completed by removal of the Boc group and formation of the urea with *tert*-butyl isocyanate.

Based on their favorable potency and metabolic stability profiles, pyridazinones **4** and **6** and pyrazolopyridines **13** and **14** were subjected to further *in vitro* profiling (Table 3). All compounds showed high protein binding. Compounds **13** and **14** showed long $T_{1/2}$ values in the presence of both human and mouse liver microsomes, while the $T_{1/2}$ of compound **4** was moderate for mouse and short for human, and the $T_{1/2}$ of compound **6** was low for both species. Pyrazolopyridine **13** was chosen for advancement into mouse PK/PD studies due to its high level of potency and metabolic stability; **4** was chosen to represent the pyridazinone series due to its greater metabolic stability relative to **6**.

At a 100 mg/kg oral dose, compound **4** showed a relatively high initial exposure (Table 4) with a $T_{1/2}$ of 1.9 h and negligible exposure at 24 h. In contrast, compound **13** had an extended absorption period with a maximum concentration at 7 h, a 5.3 h $T_{1/2}$, and substantial exposure even at 24 h after dosing. Spleens from the mice were harvested, and the level of LCK Y505 phosphorylation was measured. Mice treated with **4** showed an 87% decrease in LCK phosphorylation compared to vehicle-treated mice at 3 h, when plasma concentration was 8.7 μM. The decrease for mice treated with **13** was 88% at 6 h (close to the T_{max} of 7 h). Thus, both **4** and **13** show the anticipated effect of CSK inhibition upon oral dosing in mice.

To test whether compound **13** was able to activate T cells in a context-appropriate manner, an assay was utilized in which Chinese hamster ovary (CHO) cells were mixed with $CD4^+$ T cells.[14] Two types of cells were used: parental CHO cells and CHO cells expressing OKT, a cognate antibody for the T cell receptor. These cells were treated with compound **13** and monitored for IL-2 secretion and proliferation. The results from this experiment are summarized in Figure 5. As expected, the parental CHO cells induced a minimal response which was not increased by compound **13**. CHO cells expressing OKT induced a stronger response, which was increased in a dose-dependent fashion by **13**. At 333 nM of compound **13**, IL-2 secretion was increased by 5.7-fold; under the conditions employed, proliferation reached a maximum increase of 2-fold at 37 nM. Taken together, these results confirm the hypothesis that CSK inhibition can enhance the response of T cells to antigen stimulation.

In summary, we have developed a series of small molecule inhibitors of CSK that can serve as *in vitro* and *in vivo* tools to evaluate the potential of this target as an immuno-oncology therapy. Switching from a pyridazinone to pyrazolopyridine hinge binder gave a substantial increase in cellular potency. Metabolite identification studies enabled the strategic blocking of metabolic soft spots by the exchange of a *tert*-butyl urea for a cyano amide and fluorination of an indazole, culminating in the

DOI: 10.1021/acsmedchemlett.9b00354
ACS Med. Chem. Lett. 2019, 10, 1486−1491

discovery of compound **13**. Compound **13** reduced inhibitory LCK phosphorylation *in vivo* upon oral dosing and showed the ability to enhance T cell activation in response to antigen stimulation. Notably, this increase was not observed in the absence of an antigen. These findings support further evaluation of the potential of CSK inhibition to enhance antitumor immune response. The molecules described in this manuscript provide suitable tools to evaluate the relationship between the extent and duration of CSK inhibition and the efficacy and tolerability of treatment in animal models, an important consideration given the toxicity observed in knockout mice.[15,16]

■ ASSOCIATED CONTENT

Supporting Information

The Supporting Information is available free of charge on the ACS Publications website at DOI: 10.1021/acsmedchemlett.9b00354.

Experimental procedures and characterization data for the compounds described (PDF)

■ AUTHOR INFORMATION

Corresponding Author

*E-mail: daniel.o'malley@bms.com.

ORCID

Daniel P. O'Malley: 0000-0003-4420-3515

Author Contributions

All authors have given approval to the final version of the manuscript.

Funding

This work was funded by Bristol-Myers Squibb Company.

Notes

The authors declare the following competing financial interest(s): The authors of this manuscript are employees of Bristol-Myers Squibb.

■ ACKNOWLEDGMENTS

The authors wish to acknowledge the contributions of the CSK Discovery Working Group.

■ ABBREVIATIONS

CHO, Chinese hamster ovary; CTLA-4, cytotoxic T lymphocyte-associated protein 4; dppf, 1,1′-bis-(diphenylphosphino)ferrocene; HATU, 1-[Bis-(dimethylamino)methylene]-1*H*-1,2,3-triazolo[4,5-*b*]-pyridinium 3-oxide hexafluorophosphate; HTRF, homogeneous time-resolved fluorescence; LCK, lymphocyte-specific protein tyrosine kinase; PD, pharmacodynamics; PD-1, programmed cell death protein 1; PD-L1, programmed death-ligand 1; PK, pharmacokinetics; PyBOP, (benzotriazol-1-yloxy)tripyrrolidinophosphonium hexafluorophosphate; ZAP-70, zeta-chain-associated protein kinase 70

■ REFERENCES

(1) Lonberg, N.; Korman, A. J. Masterful antibodies: Checkpoint blockade. *Cancer Immunol. Res.* **2017**, *5*, 275−281.

(2) Adams, J. L.; Smothers, J.; Srinivasan, R.; Hoos, A. Big opportunities for small molecules in immuno-oncology. *Nat. Rev. Drug Discovery* **2015**, *14*, 603−622.

(3) Toogood, P. L. Small molecule immuno-oncology therapeutic agents. *Bioorg. Med. Chem. Lett.* **2018**, *28*, 319−329.

(4) Thill, P. A.; Weiss, A.; Chakraborty, A. K. Phosphorylation of a tyrosine residue on Zap70 by Lck and its subsequent binding via an SH2 domain may be a key gatekeeper of T cell receptor signaling *in vivo*. *Mol. Cell. Biol.* **2016**, *36*, 2396−2402.

(5) Okada, M.; Nada, S.; Yamanishi, Y.; Yamamoto, T.; Nakagawa, H. CSK: a Protein-tyrosine kinase involved in regulation of *src* family kinases. *J. Biol. Chem.* **1991**, *266*, 24249−24252.

(6) Mustelin, T.; Tasken, K. Positive and negative regulation of T-cell activation through kinases and phosphatases. *Biochem. J.* **2003**, *371*, 15−27.

(7) Okada, M. Regulation of the Src family kinases by Csk. *Int. J. Biol. Sci.* **2012**, *8*, 1385−1397.

(8) Vang, T.; Abrahamsen, H.; Myklebust, S.; Enserink, J.; Prydz, H.; Mustelin, T.; Amarzguioui, M.; Tasken, K. Knockdown of C-terminal Src kinase by siRNA-mediated RNA interference augments T cell receptor signaling in mature T cells. *Eur. J. Immunol.* **2004**, *34*, 2191−2199.

(9) Manz, B. N.; Tan, Y. X.; Courtney, A. H.; Rutaganira, F.; Palmer, E.; Shokat, K. M.; Weiss, A. Small molecule inhibition of Csk alters affinity recognition by T cells. *eLife* **2015**, *4*, No. e08088.

(10) Sheppard, K.-A.; Fitz, L. J.; Lee, J. M.; Benander, C.; George, J. A.; Wooters, J.; Qiu, Y.; Jussif, J. M.; Carter, L. L.; Wood, C. R.; Chaudhary, D. PD-1 inhibits T-cell receptor induced phosphorylation of the ZAP70/CD3 signalosome and downstream signaling to PKC. *FEBS Lett.* **2004**, *574*, 37−41.

(11) Yokosuka, T.; Takamatsu, M.; Kobayashi-Imanishi, W.; Hashimoto-Tane, A.; Azuma, M.; Saito, T. Programmed cell death 1 forms negative costimulatory microclusters that directly inhibit T cell receptor signaling by recruiting phosphatase SHP2. *J. Exp. Med.* **2012**, *209*, 1201−1217.

(12) For a report of a CSK inhibitor with an IC_{50} of 1.9 μM in an ELISA assay, see: Kilimnik, A.; Kostjukova, M. N.; Pyatkin, I. H.; Pronin, A. M.; Strelnikova, S. R.; Fedotov, Y. A.; Kolesnikov, A. V. Novel small-molecule inhibitors of C-terminal Src Kinsase (Csk). *Cell. Mol. Biol. Lett.* **2003**, *8*, 588.

(13) Paiva, A. A.; Klakouski, C.; Li, S.; Johnson, B. M.; Shu, Y.-Z.; Josephs, J.; Zvyaga, T.; Zamora, I.; Shou, W. Z. Development, optimization, and implementation of a centralized metabolic soft spot assay. *Bioanalysis* **2017**, *9*, 541−552.

(14) For application of a similar assay, see: Englehardt, J. J.; Selby, M. J.; Korman, A. J.; Feingersh, M. D.; Stevens, B. L. *Anti-Icos agonist antibodies and uses thereof*. WO 2018/187613 A2, October 11, 2018.

(15) For additional studies on a different series of CSK inhibitors from this group, see: Wang, C.; Cao, C.; Berman-Booty, L.; Eraslan, R.; Sanjuan, M.; Vite, G.; Hunt, J.; Fink, B.; Wee, S. Targeting CSK kinase activity to enhance antitumor immunity [abstract]. *Proceedings of the AACR Special Conference on Tumor Immunology and Immunotherapy*; 2017 Oct 1−4; AACR, Boston, MA. Philadelphia (PA). *Cancer Immunol. Res.* **2018**, *6* (9 Suppl), Abstract nr B02.

(16) Berman-Booty, L. D.; Eraslan, R.; Hanumegowda, U.; Cantor, G. H.; Bounous, D. I.; Janovitz, E. B.; Jones, B. K.; Buiakova, O.; Hayward, M.; Wee, S. Systemic loss of C-terminal Src kinase expression elicits spontaneous suppurative inflammation in conditional knockout mice. *Vet. Pathol.* **2018**, *55*, 331−340.

DOI: 10.1021/acsmedchemlett.9b00354
ACS Med. Chem. Lett. 2019, 10, 1486−1491